

Magnetic Properties and Low-Field ESR of Organic Free Radicals, Monochloroporphyrin and Porphyrin

Toshio YOSHIOKA*

Department of Chemistry, Faculty of Science, Kyoto University, Sakyo-ku, Kyoto 606

(Received August 9, 1976)

The static magnetic susceptibility, and ESR and proton NMR spectra of powder samples of monochloroporphyrin were measured above 1 K and compared with those of porphyrin. A broad maximum in the static susceptibility of monochloroporphyrin, indicating an antiferromagnetic interaction, appeared at 22.5 K. The relative susceptibilities of the two radicals obtained from the ESR signal intensities and the proton NMR shifts agree qualitatively with the static susceptibilities. In the low-field ESR spectra (135 MHz) of each radical, broadening of the $g=2$ absorption line and distinct appearance of the $g=4$ absorption line were found in the temperature region below T_m , the temperature at which the susceptibility is maximum. The anisotropy of the g -value was estimated from Q-band ESR spectra. Furthermore, the unpaired electron-spin distribution over the ring was estimated from the X-band ESR and the proton NMR spectra. The results are interpreted assuming that the magnetic behavior of the two radicals is due to alternating antiferromagnetic Heisenberg linear chains with alternating parameters, $a=0.4$ and $a=0.6$, respectively.

At low temperatures, the magnetic susceptibility of many stable neutral radicals deviates from the Curie-Weiss law and sometimes has a broad maximum which indicates the presence of an antiferromagnetic exchange interaction J between unpaired electrons of the radicals.¹⁻⁵ This anomalous magnetic behavior has been interpreted in terms of the one-dimensional Heisenberg model with an antiferromagnetic exchange interaction.³ Such an interaction is considered to be due to the overlap of the $2p_z\pi$ -orbitals, each of which is occupied by an unpaired electron, and the one-dimensionality may be caused by the uniaxial characteristic of the π -orbital. It has been reported in previous papers, however, that for the porphyrin radical the magnetic behavior is different from that for 2,2,6,6-tetramethyl-4-hydroxypiperidine-1-oxyl (TANOL), which is a one-dimensional Heisenberg antiferromagnet typical of organic neutral radicals.^{3,4} Its magnetic susceptibility is better interpreted using the Ising model rather than the linear Heisenberg model. The difference between the magnetic properties of TANOL and porphyrin has been considered to be due to their different molecular structures; the former has a non-planar molecular framework and a localized spin distribution, while the latter is somewhat planar with the unpaired electron expected to be over the ring. In order to clarify the magnetic properties of porphyrin radicals, a chloroderivative of porphyrin has been chosen as an appropriate sample. In this paper, the results of the magnetic susceptibility and ESR and

proton NMR measurements of monochloroporphyrin (Cl-porphyrin) are reported for temperatures above 1 K, and the exchange interaction, spin correlation, and unpaired electron-spin distribution in porphyrin radicals are discussed by comparing the results with those of porphyrin and TANOL. Cl-porphyrin has been suggested to have the molecular structure shown in Fig. 1.⁶

Experimental

The porphyrin radical was obtained commercially and was used without further purification. The sample of monochloroporphyrin was prepared according to the procedure of Piloty and Schwerin,⁷ and was purified by recrystallization from methanol, mp 151—152 °C. The results of elemental analysis correspond closely to the calculated values. Found: C, 34.42; H, 4.61; N, 31.99; Cl, 20.10%. Calcd for $C_8H_8N_4OCl$: C, 34.18; H, 4.56; N, 31.91; Cl, 20.22%. TANOL was prepared by the oxidation of 2,2,6,6-tetramethyl-4-hydroxypiperidine according to the process of Rozantsev,⁸ and was purified by recrystallization.

The magnetic susceptibilities were measured for powder samples of about 80 mg in a field of 8.8 kG from 1.7 to 300 K by means of a magnetic torsion balance described elsewhere.⁹ The temperatures were measured with an AuCo-Cu thermocouple and a carbon resistor calibrated by measuring not only the magnetic susceptibility of Mn-Tutton salt, but also the vapor pressures of liquid helium, liquid hydrogen, and liquid nitrogen. The proton NMR measurements were carried out using a Robinson-type spectrometer operating at 35.0 MHz with an 80-Hz field modulation and with a field sweep. The magnetic field was calibrated by means of the proton absorption of H_2O . The low-field ESR (LF-ESR) spectra were observed using a Benedek-Kusida type spectrometer at 135 MHz.¹⁰ Details of the apparatus for the low-field ESR measurements have been described elsewhere.¹¹ A conventional cryostat was used, and temperatures were determined using an Allen-Bradley carbon resistor calibrated against the vapor pressures of liquid helium, hydrogen, and nitrogen. The high-field ESR spectra in solution and in the crystalline state were obtained at room temperature, using JEOLCO X-band and Q-band spectrometers, respectively. The magnetic field was calibrated using the hyperfine splittings of Mn^{2+} doped in MgO .

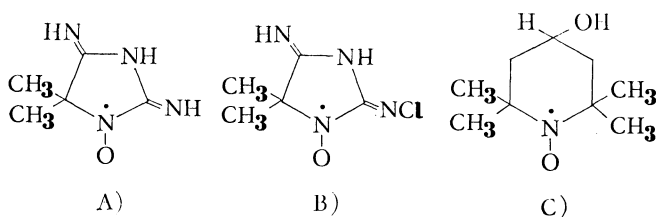


Fig. 1. Molecular structures of the radicals.

A) Porphyrin, B) Cl-porphyrin, C) TANOL.

* Present address: Fibers Research Laboratories, Toray Industries, Inc., Sonoyama, Otsu 520.

TABLE 1. RESULTS FROM SUSCEPTIBILITY MEASUREMENTS

	χ_d (10^{-4} emu/mol)	θ (K)	T_m (K)	χ_m (10^{-4} emu/mol)	p	$J/k(K)$	a
Cl-porphyraxide	-1.08	-20	22.5	72	0.96	-18.2	0.4
Porphyraxide ^{a)}	-0.85	-8	7.2	207	0.91	-5.9	0.6
TANOL ^{b)}	-1.1	-6	6.5	226	1.00	-5.0	1.0

a) Ref. 4. b) Ref. 3.

Results

Susceptibility. The diamagnetic correction was made using Pascal's constant. The diamagnetic susceptibility, χ_d , is listed in Table 1. In the temperature range above 40 K, the paramagnetic susceptibility, χ_p , of Cl-porphyraxide follows the Curie-Weiss law, with a Weiss constant of $\theta = -20$ K and a spin concentration of 96.5%. As the temperature is lowered below 40 K, it deviates from the Curie-Weiss law and reaches a broad maximum at $T_m = 22.5$ K, as is shown in Fig. 2. After passing through the maximum, it decreases gradually down to 3.5 K. However, below 3.5 K it increases again as the temperature is lowered. In the region from 1.7 to 2.3 K, the Curie-Weiss law was observed with a spin concentration of 0.5% and a Weiss constant of -0.4 K. When this low-temperature paramagnetic impurity curve is extrapolated to higher temperatures and subtracted from the experimental values, the corrected curve shown in Fig. 2 is obtained.

Proton NMR. In the proton NMR spectra of a powder sample of Cl-porphyraxide at 35.0 MHz, an assymetric single line was observed at a free proton position in the temperature range of 1.6–77 K. When the temperature was lowered below 77 K, the linewidth defined as the maximum slope width of signals obtained

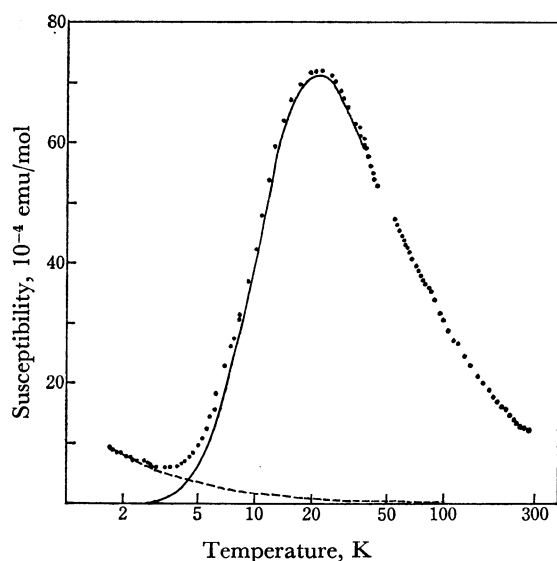


Fig. 2. Paramagnetic molar susceptibility of Cl-porphyraxide radical. The full circles represent the experimental values. The impurity curve indicated by the broken line is an extrapolation of the low temperature Curie-Weiss data. The solid line shows the difference between the experimental values and the impurity curve.

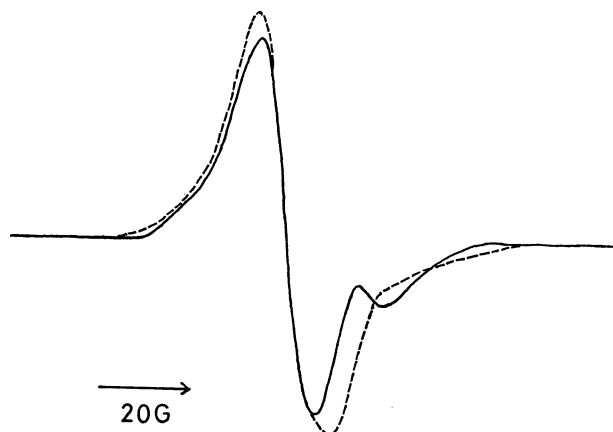


Fig. 3. Proton magnetic resonance spectra of porphyraxide, measured at 35 MHz. The solid line and the broken line represent the spectra at 20 K and 4.2 K, respectively.

by 80-Hz field modulation increased and reached a maximum value of 8.0 G in the vicinity of $T_m = 22.5$ K. Below T_m , it decreased as the temperature was lowered, and reached a value of 5.5 G at 4.2 K.

The proton NMR spectra of a powder sample of porphyraxide at 35.0 MHz are shown in Fig. 3. In addition to the central unshifted line, one more absorption line shifted to higher magnetic field was observed in the temperature region 3.0–30 K. The magnitude of the shift was largest in the vicinity of $T_m = 7.6$ K.⁴⁾ The resonance field of the unshifted line almost corresponded to the magnetic field of a free proton at that frequency.

X-Band ESR in Solution. The X-band ESR spectrum of Cl-porphyraxide in a chloroform solution is shown in Fig. 4. Triplet splitting ($a_N = 8.5$ G), caused by the hyperfine interaction between an unpaired electron and a ^{14}N nucleus, and several subsplittings are observed. The g -value of Cl-porphyraxide in solution was determined to be 2.0060, which coincides with the values of other nitroxide radicals.



Fig. 4. The X-band ESR spectrum of Cl-porphyraxide in a chloroform solution.

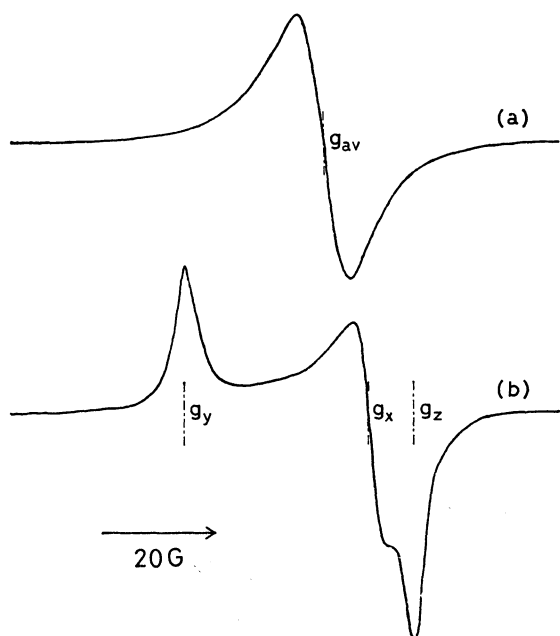


Fig. 5. The Q-band ESR spectra of porphyrin (a) and Cl-porphyrin (b) measured at room temperature.

Q-Band ESR. The Q-band ESR spectra for powder samples of porphyrin and Cl-porphyrin measured at room temperature are shown in Figs. 5(a) and (b), respectively. A relatively symmetrical single line was observed for porphyrin. On the other hand, the spectrum of Cl-porphyrin consists of three peaks. When single crystals of Cl-porphyrin were used, a single line was obtained for any crystal orientation; the resonance field exhibited an angular dependence for an external magnetic field applied in a certain plane.

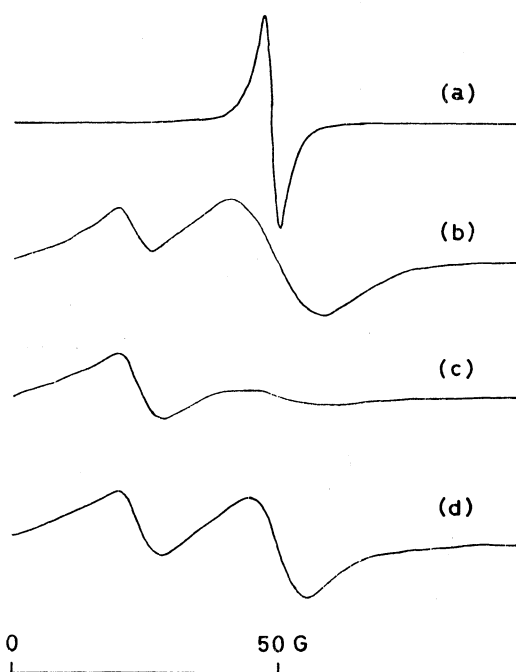


Fig. 6. The LF-ESR spectra of Cl-porphyrin measured at 135 MHz. (a) $T = 77$ K, (b) $T = 6.3$ K, (c) $T = 4.2$ K, (d) $T = 2.0$ K.

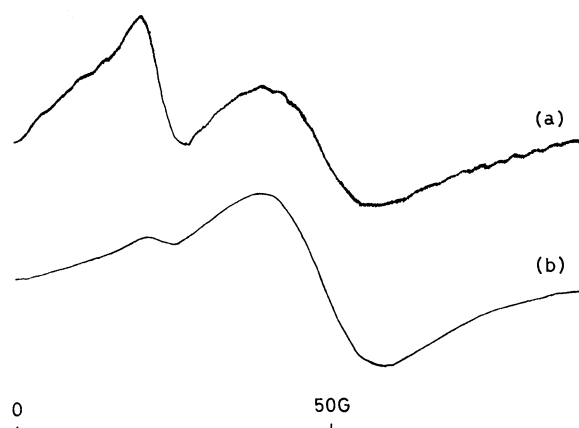


Fig. 7. The LF-ESR spectra of porphyrin (a) and TANOL (b) measured at 135 MHz and at 1.4 K.

LF-ESR. The LF-ESR absorption spectra of powder samples of Cl-porphyrin, porphyrin, and TANOL all exhibit a single line which has an exchange-narrowed Lorentzian shape at room temperature. The temperature dependence of the LF-ESR spectrum for Cl-porphyrin is shown in Fig. 6. Figures 7(a) and (b) show the LF-ESR spectra of porphyrin and TANOL, respectively, measured at 1.4 K. When the temperature was lowered below room temperature, the linewidth of the $g=2$ absorption, defined as the peak-to-peak linewidth of the first derivative of the absorption spectrum, gradually decreased and exhibited a minimum in the vicinity of T_m . Then, it started to increase rapidly as the temperature was further decreased. Cl-porphyrin and porphyrin linewidths decreased again below given temperatures. The temperature dependence

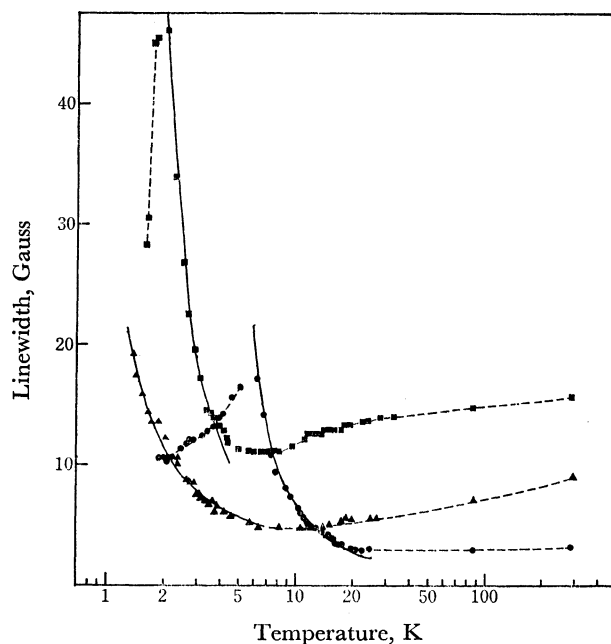


Fig. 8. The temperature dependence of the LF-ESR linewidth. —●—, Cl-porphyrin, —■— porphyrin, —▲— TANOL. The solid lines represent the curves calculated by Eq. 6.

of the linewidth for each sample is shown in Fig. 8. The relative susceptibility, obtained from the signal intensity, agreed qualitatively with the static susceptibility; it could not be treated quantitatively since the spectrometer sensitivity changed with temperature. The $g=4$ absorption could not be observed at room temperature or at liquid nitrogen temperature. Below the temperature at which the susceptibility deviated from the Curie-Weiss law, the $g=4$ ESR absorption was detected as the temperature was lowered. The linewidth of the $g=4$ ESR absorption was independent of the temperature within the experimental error. The ratio of the peak intensity of the $g=4$ resonance absorption to that of the $g=2$ absorption depended upon the angle between the direction of the radio-frequency field and that of the static magnetic field; it was the smallest when the radio-frequency field and the static magnetic field were perpendicular to each other.

Discussion

Susceptibility. The behavior of the magnetic susceptibility of Cl-porphyrin is very similar to that of porphyrin,⁴⁾ although the temperature T_m for the former is almost three times as high as that for the latter. The magnetic behavior cannot be explained quantitatively by the well-known pair model described by:

$$\chi_p = (Ng^2\beta^2S(S+1)/3kT)[1 + (1/3) \exp(\Delta/kT)]^{-1}, \quad (1)$$

where Δ is the energy splitting between the ground singlet and the excited triplet states and is equal to $2J$. The maximum value of the observed susceptibility, χ_m , is about 15% smaller than the theoretical value calculated from Eq. 1. Moreover, the experimental values deviate from the theoretical χ_p - T curve as the temperature is decreased below T_m . These discrepancies can be reduced by introducing the alternating antiferromagnetic Heisenberg linear chain model¹²⁾ or the anisotropic regular chain model.¹³⁾ The susceptibility data of the nitroxide radical, TANOL, has been analyzed successfully on the basis of the regular Heisenberg model.³⁾ In the case of Cl-porphyrin and porphyrin, the g -values are nearly isotropic and are similar to those of nitroxide radicals, as is shown below, so that it is not appropriate to discuss their magnetic properties on the basis of the latter model. Therefore, the susceptibility data have been analyzed using the former model. The spin Hamiltonian for the former model is given by:

$$\mathcal{H} = -2J \sum_{i=1}^{N/2} (S_{2i} \cdot S_{2i-1} + a S_{2i} \cdot S_{2i+1}), \quad (2)$$

where J is the exchange integral coupling a certain spin with its nearest neighbor and aJ is the exchange integral of a spin with its next nearest neighbor. This model corresponds to the pair model when $a=0$ and to the regular Heisenberg model when $a=1$. The exact eigenvalue spectrum and thermodynamic properties of Eq. 2 have been calculated for short chains by Duffy and Barr.¹²⁾

In Fig. 9, the (χ_p/p) - T data for Cl-porphyrin and porphyrin are given together with the "best fit"

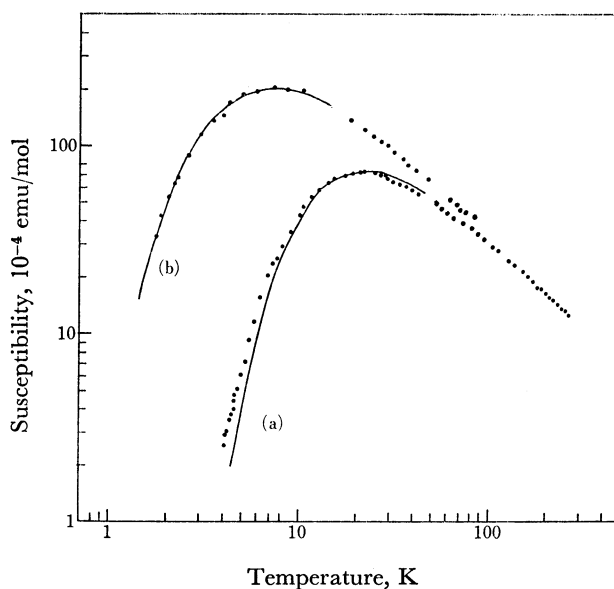


Fig. 9. Magnetic molar susceptibilities of Cl-porphyrin (a) and porphyrin (b). The full circles represent the experimental values of χ_p/p . The solid lines represent the theoretical χ_p - T curves with $a=0.4$ and $J/k=-18.2$ K (a), and $a=0.6$ and $J/k=-5.9$ K (b).

theoretical curves with $a=0.4$ and $J/k=-18.2$ K, and $a=0.6$ and $J/k=-5.9$ K, respectively. Here, p is the spin concentration which was found from the Curie-Weiss law observed at high temperature and is given in Table 1. The theoretical curves for $N=10$ were used, since it has been reported that the 10-spin chain values and ∞ -spin chain estimates differ by less than 0.5% at $kT/|J| > 0, 0.65, \text{ and } 0.80$ for $a=0.2, 0.4, 0.6, \text{ and } 0.8$, respectively. The experimental results are in fairly good agreement with the theoretical curves. The interpretation based on this model may be tentative due to lack of a detailed crystal-structure determination. However, it may be concluded that the deviation of the susceptibility data from the pair-model curve is probably due to the existence of the second-strongest exchange interaction, since the curve for the pair model is described only by the strongest exchange interaction. The resulting parameters are summarized in Table 1, together with those for TANOL. The exchange parameter J for Cl-porphyrin is relatively large in comparison with those of other neutral organic radicals and is the largest of the ring-iminoxyl radical exchange parameter investigated. The rise in the susceptibility of Cl-porphyrin below 3.5 K is attributable to the impurity effect, as no abnormal behavior in the proton NMR spectra was found in this temperature range.

Recent specific heat and proton magnetic resonance measurements below 1 K, in the case of TANOL, revealed that the magnetic-phase transition occurs at about 0.4 K.^{14,15)} On the other hand, it may be impossible for Cl-porphyrin and porphyrin to change into a long-range ordered state even if the temperature is lowered below 1.4 K, since the magnitude of the susceptibilities is so small at 1.4 K that the exchange interaction leading to a long-range ordered state, such

as the interchain exchange interaction, is no longer effective.

Proton NMR. In the polycrystalline samples, the proton-resonance signal shift from the free-proton position in the direction of higher field can be approximately described by the following equation:^{16,17)}

$$\delta H = -a_H \chi H / g \beta g_N \beta_N. \quad (3)$$

The paramagnetic shift, δH , is proportional to the hyperfine coupling constant, a_H , and to the static magnetic susceptibility per molecule, χ . Taking the molecular framework of porphyrin into account, the absorption line shifted to higher field can be roughly attributed to the three protons attached to the nitrogen atoms and the unshifted line to the six protons of the two methyl groups, since the spin density of the carbon atoms attached to the two methyl groups is expected to be very small. The hyperfine coupling constants of the three protons are evaluated to be -2.5 G using the susceptibility results.⁴⁾ From McConnell's relation, the unpaired electron-spin densities of the three nitrogen atoms are estimated to be $+0.074$ using $Q(\text{NH}) = -33.7$ as obtained by Barton and Frenkel.¹⁸⁾ This assignment may be valid since the sign of the spin densities of the three nitrogen atoms is expected to be positive on the basis of electronic structure.

The resolved spectrum of Cl-porphyrin could not be observed, since the static susceptibility is relatively small even at T_m . However, the asymmetric line shape may be due to the existence of a hyperfine interaction between the unpaired electron and the two protons attached to the nitrogen atoms. The temperature dependence of the linewidth may be explained by the hyperfine interaction which is related to the static susceptibility.¹⁷⁾ The susceptibility of TANOL obtained from the proton NMR shifts in single crystals agrees quantitatively with that of the one-dimensional Heisenberg model.¹⁹⁾

X-Band ESR in Solution. The ^{14}N hyperfine constants, a_N , obtained in solution are shown in Table 2.^{20,21)} The hyperfine constants arising from the nitrogen nucleus of the NO group can be semiempirically described by the following equation:^{22,23)}

$$a_N = 134.8\rho_N - 35.8\rho_O, \quad (4)$$

where ρ_N and ρ_O are the unpaired π -electron spin

TABLE 2. HYPERFINE CONSTANTS AND SPIN DENSITIES

	$a_N(\text{G})$	ρ_N	ρ_O
TANOL	15.5 ^{a)}	0.30	0.70
Porphyrin	10.0 ^{b)}	0.22	0.56
Cl-porphyrin	8.5	0.20	0.51

a) Ref. 20. b) Ref. 21.

densities at the nitrogen and oxygen atoms. In TANOL the values of $\rho_N + \rho_O$ is considered to be 1.0 since the unpaired electron is almost localized on the NO group masked by the four methyl groups. In porphyrin the value of $\rho_N + \rho_O$ is estimated to be 0.78 using the NMR results neglecting the spin densities of the two carbon atoms attached to the nitrogen atoms which are expected to be negative and small on the basis of the electronic structure. Therefore, ρ_N and ρ_O were calculated from Eq. 4. In Cl-porphyrin, they were calculated assuming that the value of ρ_N/ρ_O is equal to that of porphyrin. The results are summarized in Table 2. The NMR and ESR results indicate that, in porphyrin radicals, 20–30% of the unpaired electron from the NO group is distributed over the ring. Delocalization of the unpaired electron over the ring may play some role in the exchange interaction. Furthermore, it may be related to the high stabilization of these radicals, in addition to the steric hindrance of the two methyl groups.

Q-Band ESR. The Q-band ESR spectrum for powder samples of Cl-porphyrin can be interpreted in terms of the g -factor anisotropy. The principal g -values obtained using the approximation of Kneubühl²⁴⁾ are shown in Table 3. Kikuchi has calculated the g -values of several nitroxide radicals using the CNDO/2 molecular-orbital calculation method.²⁵⁾ The calculated principal g -values of H_2NO are cited in Table 3, along with the principal axes given by Kikuchi. The principal values are in fairly good agreement with those of Cl-porphyrin. Furthermore, in the case of single crystals crystallized from methanol in rhombic plates, a single line was obtained for any crystalline orientation. These facts indicate that probably all the Cl-porphyrin radicals are oriented with the N–O bond aligned along a unique direction in the crystalline state even if there is more than one site per unit cell. One-site ESR spectra were observed in the case of TANOL, as is expected from its crystal structure.²⁶⁾ The principal values are also given in Table 3.

On the other hand, a relatively symmetrical single line was observed for porphyrin, with $g = 2.0060$ which corresponds to the averaged g -value for the nitroxide radicals. The porphyrin molecules have at least two different orientations in the crystalline state, so that the g -factor anisotropy may be averaged out by the exchange interaction between the unpaired electrons of two molecules oriented differently. The fact that Cl-porphyrin has a large exchange interaction compared with that of porphyrin can be ascribed to the difference in the crystal structure. The strongest exchange interaction of Cl-porphyrin may arise from the overlap of the $p_z\pi$ -orbitals between adjacent molecules

TABLE 3. PRINCIPLE AND AVERAGED g -VALUES

	g_x	g_y	g_z	g_{av}	Axis
Cl-porphyrin	2.0048	2.0098	2.0034	2.0060	
Porphyrin	—	—	—	2.0061	
TANOL	2.0064	2.0096	2.0027	2.0062	
$\text{H}_2\text{NO}^a)$	2.0062	2.0091	2.0023	2.0059	

a) Calculated values (Ref. 25).

aligned in the z -direction. The decrease in the strongest exchange interaction of porphyraxide in comparison with that of Cl-porphyraxide is considered to be due to the increase in the distance between the two molecules or to the twisted overlap of the $P_z\pi$ -orbitals, which is caused by the existence of more than two molecular orientations.

LF-ESR. In the case of powder samples, the LF-ESR linewidths are more important since the contribution to the linewidth from the anisotropy of the g -values is excluded. The absorption lines observed at room temperature exhibit exchange-narrowed Lorentzian shapes. We can apply the usual three-dimensional Anderson-Weiss formula for a Lorentzian line:²⁷⁾

$$\Delta H = \Delta H_d^2 / \sqrt{3} H_{ex}, \quad (5)$$

where ΔH is the peak-to-peak linewidth, ΔH_d^2 the second moment of the sum of the dipole-dipole interactions that would be observed in the absence of exchange, and H_{ex} the exchange field which is directly proportional to the exchange interaction J . In the low-field case, the so-called 10/3 effect is taken into account in Eq. 5. Since the crystal structures of Cl-porphyraxide and porphyraxide have not been determined, the second moment cannot be estimated from the Van Vleck formula. However, the second moment is the sum of the dipole-dipole interactions within the crystal, so that it is not as sensitive to changes in the crystal structure as is the exchange interaction. Therefore, the ratio of the exchange integrals J of Cl-porphyraxide and porphyraxide are evaluated from the ESR linewidths at 290 K and T_m to be 4.7 and 3.7, respectively, provided that the second moment of Cl-porphyraxide is approximately equal to that of porphyraxide. This ratio is consistent with the ratio 3.1 obtained from the magnetic susceptibility results (Table 1). This suggests that the ESR lines are narrowed predominantly by the strongest exchange interaction in the high-temperature range.

TABLE 4. PARAMETERS FOR TEMPERATURE DEPENDENT LF-ESR LINEWIDTH: $\Delta H = \alpha \exp(\beta J/kT)$

	α	β
Cl-porphyraxide	1.1	0.93
Porphyraxide	3.0	0.95
TANOL	3.6	0.48

The decrease in the linewidth from room temperature to T_m may be interpreted in terms of the contribution of spin-lattice relaxation to the linewidth since the spin-lattice relaxation time generally increases with decreasing temperature. The rapid broadening of the resonance is attributable to an increase in the correlation time for exchange motion because of spin ordering below the temperature of maximum susceptibility. As is shown in Fig. 7, the observed linewidth versus temperature below T_m can be fitted to the following empirical relation:

$$\Delta H = \alpha \exp(\beta J/kT). \quad (6)$$

The α and β values are summarized in Table 4. The β value is considered to be associated with the correlation

mechanism of exchange motion which may be related to the magnetic behavior of the system. It is interesting that the β value for Cl-porphyraxide is roughly equal to that for porphyraxide and is almost twice as large as that for TANOL. These results indicate that the magnetic behavior of Cl-porphyraxide is similar to that of porphyraxide in spite of the difference in the crystal structures expected on the basis of the Q-band ESR spectra and is different from that of TANOL. Furthermore, they suggest that the exchange correlation time increases more rapidly in a pair-like system such as an alternating linear-chain system than in a regular linear-chain system. The narrowing of the resonance line below a certain temperature is probably due to paramagnetic impurities. Such behavior was also found in PAC and in Würster's blue perchlorate.²⁸⁾

The resonance line at $g=4$ is not due to the $\Delta M=2$ transition within the triplet levels caused by pairs of exchange coupling spins, since it has been found even for TANOL, in which no electron spin pairing occurs. It is probably caused by a forbidden transition due to dipolar interaction, as has been reported by Rhodes *et al.*²⁹⁾ In the high-temperature region, the strong exchange interaction averages the dipolar coupling, so that the $g=4$ resonance cannot be detected.²⁹⁾ The appearance of the $g=4$ resonance at low temperatures can be explained by an increase in the correlation time for exchange motion, as is expected from the linewidth of the $g=2$ resonance and the susceptibility data.

Summary

Because of the isotropic character of the g -factor, the susceptibility of Cl-porphyraxide was interpreted assuming that the magnetic behavior is due to alternating antiferromagnetic Heisenberg linear chains. The parameters derived from the susceptibility are $\theta = -20$ K, $T_m = 22.5$ K, $\chi_m = 72 \times 10^{-4}$ emu/mol, $J/k = -18.2$ K, and $a = 0.4$. The fact that the strongest exchange interaction for Cl-porphyraxide is almost three times as large as that for porphyraxide is considered to be due to the difference of the crystal structures, as is expected from the Q-band ESR spectra. The LF-ESR lines are narrowed by the exchange interaction in the high-temperature region and the ratio of the strongest exchange integral J for Cl-porphyraxide to that for porphyraxide obtained from the linewidth is consistent with the ratio obtained from the susceptibility data. The rapid broadening of the $g=2$ absorption line and the distinct appearance of the $g=4$ absorption line are attributable to an increase in the correlation time for exchange motion resulting from spin ordering below the temperature of the susceptibility maximum. The susceptibility data and the temperature dependence of the LF-ESR linewidths indicate that the magnetic behavior of Cl-porphyraxide is similar to that of porphyraxide and is different from that of TANOL. In porphyraxide radicals, 20–30% of the unpaired electron is distributed over the ring from the NO group. More quantitative discussions concerning the magnetic interaction will be possible when detailed crystal-structure determinations are available in the future.

The author is deeply indebted to Professor Yasuo Deguchi for his continuous encouragement throughout this work, and also to Drs. Hiroaki Ohya-Nishiguchi, Jun Yamauchi, and Akira Nakajima for helpful advice and discussions. He also thanks Mr. Teruaki Fujito for supplying the susceptibility data of porphyrexide. Thanks are also due to Dr. Kohji Watanabe for his advice on the preparation of the samples.

References

- 1) W. Duffy, Jr., and D. L. Standburg, *J. Chem. Phys.*, **46**, 456 (1967).
- 2) W. Duffy, Jr., and K. P. Barr, *Phys. Rev.*, **165**, 647 (1968).
- 3) J. Yamauchi, *Bull. Chem. Soc. Jpn.*, **44**, 2301 (1971).
- 4) T. Fujito, H. Nishiguchi, Y. Deguchi, and J. Yamauchi, *Bull. Chem. Soc. Jpn.*, **42**, 3334 (1969).
- 5) N. Azuma, J. Yamauchi, K. Mukai, and H. Ohya-Nishiguchi, *Bull. Chem. Soc. Jpn.*, **46**, 2728 (1973).
- 6) A. R. Forrester, J. M. Hay, and R. H. Thomson, "Organic Chemistry of Stable Free Radicals," Academic Press, London (1968), p. 227.
- 7) O. Piloty and B. G. Schwerin, *Ber.*, **34**, 2354 (1901).
- 8) E. G. Rozantsev, *Izv. Akad. Nauk. SSSR, Ser. Khim.*, **12**, 2218 (1964).
- 9) H. Mekata, *J. Phys. Soc. Jpn.*, **17**, 796 (1962).
- 10) G. B. Benedek and T. Kusida, *Phys. Rev.*, **118**, 46 (1960).
- 11) M. A. Garstens, L. S. Singer, and A. H. Ryan, *Phys. Rev.*, **96**, 53 (1954).
- 12) W. Duffy, Jr., and K. P. Barr, *Phys. Rev.*, **96**, 53 (1954).
- 13) J. C. Bonner and N. E. Fisher, *Phys. Rev. A*, **135**, 640 (1964).
- 14) S. Saito and T. Sato, *Phys. Lett. A*, **44**, 2301 (1971).
- 15) J. P. Boucher, M. Hechtschein, and M. Saint-Paul, *Phys. Lett. A*, **42**, 397 (1972).
- 16) T. Yoshioka, H. Ohya-Nishiguchi, and Y. Deguchi, *Bull. Chem. Soc. Jpn.*, **47**, 430 (1974).
- 17) T. Yoshioka, K. Watanabe, and H. Ohya-Nishiguchi, *Bull. Chem. Soc. Jpn.*, **48**, 2533 (1975).
- 18) B. L. Barton and G. K. Frenkel, *J. Chem. Phys.*, **41**, 1455 (1964).
- 19) T. Yoshioka, unpublished work.
- 20) K. Watanabe, J. Yamauchi, H. Takaki, H. Nishiguchi, and Y. Deguchi, *Bull. Inst. Chem. Res., Kyoto Univ.*, **48**, 264 (1970).
- 21) K. H. Hausser, *Z. Naturforsch.*, **14a**, 425 (1959).
- 22) K. Mukai, H. Nishiguchi, K. Ishizu, Y. Deguchi, and H. Takaki, *Bull. Chem. Soc. Jpn.*, **40**, 2731 (1967).
- 23) P. H. Rieger and G. K. Fraenkl, *J. Chem. Phys.*, **39**, 609 (1963).
- 24) F. K. Kneubühl, *J. Chem. Phys.*, **33**, 1074 (1960).
- 25) O. Kikuchi, *Bull. Chem. Soc. Jpn.*, **40**, 704 (1967).
- 26) J. Lajzerowicz-Bonnateau, *Acta Crystallogr. Sect. B*, **24**, 196 (1968).
- 27) P. W. Anderson and P. R. Weiss, *Rev. Mod. Phys.*, **25**, 269 (1953).
- 28) R. S. Rhodes, J. H. Burgess, and A. S. Edelstein, *Phys. Rev. Lett.*, **6**, 462 (1961).
- 29) V. I. Kononov and S. M. Ryabchenko, *Soviet Physics-Solid State*, **8**, 2833 (1967).